

CONF-9609295--1

RECEIVED

NOV 01 1996

OSTI

Self-Excited Induction Generator for Variable-Speed Wind Turbine Generation

E. Muljadi, B. Gregory, D. Broad
National Renewable Energy Laboratory

*Prepared for
POWERSYSTEMS WORLD '96 Conference
Ventura, California
September 7-13, 1996*



MASTER

National Renewable Energy Laboratory
1617 Cole Boulevard
Golden, Colorado 80401-3393
A national laboratory of the U.S. Department of Energy
Managed by Midwest Research Institute
for the U.S. Department of Energy
under contract No. DE-AC36-83CH10093

Prepared under Task No. WE619030

October 1996

DISTRIBUTION OF THIS DOCUMENT IS UNLIMITED

A handwritten signature or mark, possibly initials, located at the bottom right of the page.

NOTICE

This report was prepared as an account of work sponsored by an agency of the United States government. Neither the United States government nor any agency thereof, nor any of their employees, makes any warranty, express or implied, or assumes any legal liability or responsibility for the accuracy, completeness, or usefulness of any information, apparatus, product, or process disclosed, or represents that its use would not infringe privately owned rights. Reference herein to any specific commercial product, process, or service by trade name, trademark, manufacturer, or otherwise does not necessarily constitute or imply its endorsement, recommendation, or favoring by the United States government or any agency thereof. The views and opinions of authors expressed herein do not necessarily state or reflect those of the United States government or any agency thereof.

Available to DOE and DOE contractors from:
Office of Scientific and Technical Information (OSTI)
P.O. Box 62
Oak Ridge, TN 37831
Prices available by calling (423) 576-8401

Available to the public from:
National Technical Information Service (NTIS)
U.S. Department of Commerce
5285 Port Royal Road
Springfield, VA 22161
(703) 487-4650



DISCLAIMER

**Portions of this document may be illegible
in electronic image products. Images are
produced from the best available original
document.**

Self-Excited Induction Generator for Variable-Speed Wind Turbine Generation

Eduard Muljadi

Brian Gregory

Diane Broad

National Renewable Energy Laboratory
1617 Cole Boulevard
Golden, CO 80401

Department of Electrical Engineering
Colorado State University
Fort Collins, CO 80523

Abstract-When an induction generator is connected to a utility bus, the voltage and frequency at the terminal of the generator are the same as the voltage and frequency of the utility. The reactive power needed by the induction generator is supplied by the utility and the real power is returned to the utility. The rotor speed varies within a very limited range, and the reactive power requirement must be transported through a long line feeder, thus creating additional transmission losses.

The energy captured by a wind turbine can be increased if the rotor speed can be adjusted to follow wind speed variations. For small applications such as battery charging or water pumping, a stand alone operation can be implemented without the need to maintain the output frequency output of the generator. A self-excited induction generator is a good candidate for a stand alone operation where the wind turbine is operated at variable speed. Thus the performance of the wind turbine can be improved.

In this paper, we examine a self-excited induction generator operated in a stand alone mode. A potential application for battery charging is given. The output power of the generator will be controlled to improve the performance of the wind turbine.

1. Introduction

An induction machine can be operated as an isolated generator with no connection to the utility supply. When connected to the utility, the reactive power needed by the induction generator is supplied by the utility. For an isolated operation, the reactive power needed by the induction generator must be compensated by a local source such as a three-phase AC capacitor [1-3] or solid-state excitation [4-7]. While the solid-state excitation provides a variable size of reactive power, the application of solid-state excitation is generally accompanied by harmonics generated by the converter and additional switching losses. The physical diagram and the per phase equivalent circuit of an induction generator in an isolated operation is presented in Fig. 1. Delta connection can also be implemented; however, for the simplicity of the analysis, a wye connected system is considered. The equivalent circuit in Fig. 2a can be generalized to account for any frequency operation,

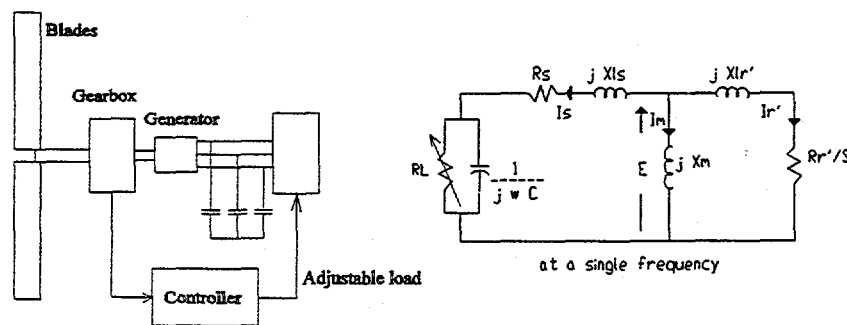


Fig. 1: Self-excited induction generator

as shown in Fig. 2b.

In an isolated operation, the conservation of real and reactive power must be preserved [8]. The equation governing the system can be simplified by looking at the impedance or admittance of the induction machine. To operate in isolated fashion, the total admittance of the induction machine must be zero. The voltage of the system is determined by the flux and frequency of the system. Thus, it is easier to start the analysis from a node at one end of the magnetizing branch. Note that the term IMPEDANCE in this paper is the conventional impedance divided by the frequency. The term ADMITTANCE in this paper corresponds to the actual admittance multiplied by the frequency.

The application of variable-speed wind turbine generation has been steadily increasing during the past ten years. The massive use of power converters in industry has also benefited the wind power developer with the possibility of using power electronics equipment to generate power at variable speed. The technical merits and economical trade-off must be considered in developing variable-speed wind turbine generation. In this paper, a low cost alternative to variable-speed wind turbine generation is explored by using a self-excited induction generation system. Compared to a permanent magnet generator, a self-excited induction generator is economically more attractive. A self-excited induction generator is controlled so that its torque-speed characteristic follows a typical variable-speed wind turbine generator (optimum power coefficient C_p). Thus if the correct choice of capacitor size can be found, and the self-excited operation of an induction generator can be matched to the wind turbine characteristic, the annual energy production of the wind turbine can be increased.

2. Equivalent Circuit

An equivalent circuit of a parallel compensated induction generator is shown in Figure 2. The principle of excitation for the parallel compensated system is the same as in the series compensation, that is, the balance of real and reactive power must be maintained. The total admittance of the system is given by

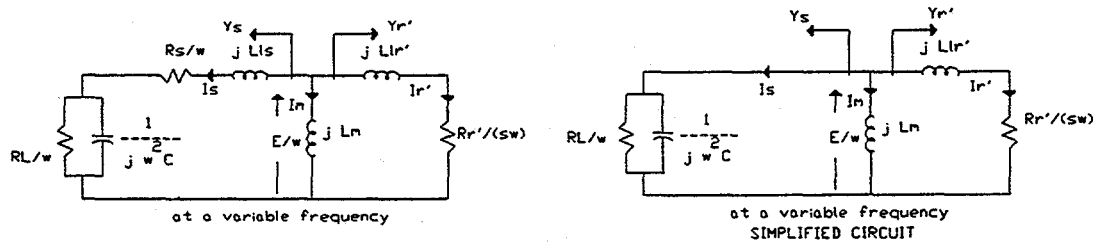


Fig. 2 : Equivalent circuit of parallel compensation
(a) variable frequency (b) simplified equivalent circuit

equation 1:

$$Y_s + Y_m' + Y_r' = 0 \tag{1}$$

The above equation can be expanded into the equation for imaginary and real parts as shown in equation 2 and equation 3.

$$\frac{\frac{R_1}{\omega} + \frac{R_r'}{S\omega}}{\left(\frac{R_1}{\omega}\right)^2 + (L_1)^2 + \left(\frac{R_r'}{S\omega}\right)^2 + L_r'^2} = 0 \quad (2)$$

$$\frac{1}{L_m'} - \frac{L_1}{\left(\frac{R_1}{\omega}\right)^2 + (L_1)^2} - \frac{L_r'}{\left(\frac{R_r'}{S\omega}\right)^2 + L_r'^2} = 0$$

$$R_1 = R_r + \frac{R_L}{((\omega CR_L)^2 + 1)} \quad (3)$$

$$L_1 = L_L + \frac{CR_L^2}{((\omega CR_L)^2 + 1)}$$

The real and imaginary parts of the admittance are given in equation 2. Thus, for a given parameter set of the induction machine and the operating frequency, the slip can be solved from the real part of the admittance.

$$a_2 S^2 + a_1 S + a_0 = 0 \quad (4)$$

where

$$a_2 = R_L L_r'^2 \omega^2 + R_r L_r'^2 \omega^2 + R_r \omega^4 R_L^2 C^2 L_r'^2$$

$$a_1 = R_r R_r' \omega^2 R_L^2 C^2 - 2 R_r' \omega^2 R_L^2 C L_r' R_r' L_r'^2 \omega^4 R_L^2 C^2$$

$$+ 2 R_r' R_L R_r R_r' L_r'^2 \omega^2 + R_r' R_L^2 + R_r' R_r^2$$

$$a_0 = R_L R_r'^2 R_r R_r'^2 + R_r \omega^2 R_L^2 C^2 R_r'^2$$

After solving the above equation for the slip, the magnetizing inductance L_m' can be solved by using equation 3. The flux level corresponding to the calculated L_m' can be found from the magnetization curve shown in appendix 2. To illustrate parallel compensation, a simplification shown in Figure 2b is assumed. The simplification is close to the actual system if the size of the stator leakage inductance and the resistor is small compared to L_m . The stator-load admittance depends solely on the load impedance. The stator admittance diagram becomes very simple and variations in the resistive load and the capacitor size can be described as straight lines. The equation governing the stator-load admittance can be written in simplified form as:

$$Y_s = \frac{\omega}{R_L} + j \omega^2 C \quad (5)$$

At a constant frequency, for a constant resistive load R_L , the operating point moves along the straight line parallel to the imaginary axis as the size of capacitor is varied. Similarly, for a constant size of capacitor, the operating point moves along the straight line as the size of the resistance load is varied.

The approach is verified by computing the equivalent circuit of an actual induction generator using actual magnetizing characteristics. The calculation results is shown in Figure 3. Each frame consists of two different curves representing two resistive load (100 ohms and 200 ohms resistors) applied at the terminal output of the generators. Figure 3a represents an ideal induction generator (R_s and $X_l = 0$) and capacitor size is 30 μF . In Figure 3b, the ideal condition is maintained and the capacitor size is increased to 60 μF to

show the effect of the capacitor size. In Figure 3c, the capacitor size is 30 μF and the actual condition is used (R_s and X_l s are the real data), to show the effect of stator leakage inductance and stator resistance.

A. Effect of Varying the Capacitor

From equation 5, it can be shown that increasing the size of the capacitor or increasing the operating frequency moves the operating point on the stator-load admittance vertically, thus increasing the imaginary part of the stator load admittance. The increment is balanced mostly by the increment of the magnetizing branch admittance, which means increasing the saturation level. Thus, at any frequency, increasing the size of the capacitor will increase the air-gap flux (i.e., the air-gap voltage and the terminal voltage). The effects can be illustrated by the airgap voltage curves (from the steady-state calculation) shown in Figure 3a and Figure 3b. As the capacitor increased from 30 μF to 60 μF , the airgap voltage increases. As the airgap voltage increases, the terminal voltage also increases and as a result the output power increases.

B. Effect of Varying the Resistive Load

The effect of varying the resistive load will move the operating point in the real axis. Thus, by increasing the load resistance, the size of the real part of the stator admittance will be reduced. Consequently, this will correspond to a lower slip and lower output power, which translates into a lower output torque. On the other hand, if the size of the resistive load is reduced, the size of the real part of the admittance will be larger, which corresponds to the higher output power and higher torque.

The effect of varying the resistive load can also be observed from the steady state calculation shown in Figure 3 in which resistive loads are set to 100 ohms or 200 ohms. As can be expected, the resistive loads does not affect the airgap voltage (flux level). However, it affects the size of output power generated. The output power is affected by the inverse of the resistive load size and airgap voltage.

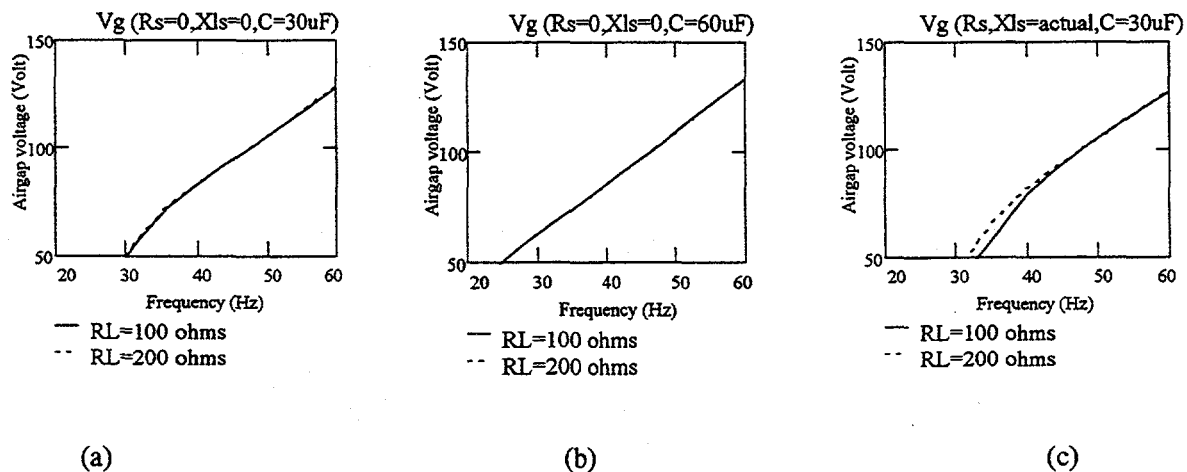


Figure 3. Effect of capacitor, resistive load, stator impedance

- Airgap voltage vs. frequency with 30 μF ac capacitor (ideal condition)
- Airgap voltage vs. frequency with 60 μF ac capacitor (ideal condition)
- Terminal voltage vs. frequency with 30 μF ac capacitor (actual condition)

C. Effect of Stator Leakage Inductance and Stator Resistance (non ideal condition)

If the actual machine parameters are used, the load resistance size can affect the airgap voltage in the lower frequency region. This effect is shown to clarify the fact that the losses in the stator winding (resistive or inductive) are more pronounced in the lower frequency region. This effect can also be shown in the

terminal voltage V_s and the output power. The larger the stator leakage and stator resistance, the larger the voltage drop, the lower the terminal voltage and the smaller the output power.

Based on the information provided in this section, we conclude that it is possible to use a self-excited induction generator to operate as a variable-speed wind turbine generator. The level of output power can be changed by changing the amount of power taken from the generator and the level of excitation can be adjusted by installing the correct size capacitor. Another parallel set of capacitors can be added to extend the operating frequency.

3. Wind Turbine Aerodynamic Characteristics

The wind turbine is normally characterized by its C_p -TSR curve as shown in Figure 4a. Where the TSR is the tip-speed ratio; that is the ratio between the linear speed of the tip of the blade with respect to the wind speed. It is shown that the power coefficient C_p varies with the tip-speed ratio. It is expected that the wind turbine is operated at high C_p values most of the time. In a fixed frequency application, the rotor-speed of the generator varies within a few percents (based on the slip) above the synchronous speed while the speed of the wind may vary across wide range.

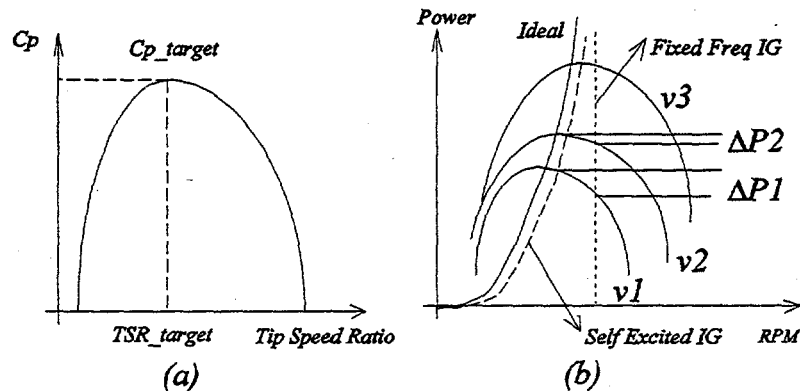


Figure 4: a) Typical C_p -TSR Curve of a Wind Turbine
b) Power vs RPM

Thus from the equation given above, the tip-speed ratio may vary from 0 to 20 depending on the turbine design. The power captured by the wind turbine may be written as

$$P_{max} = 0.5 \cdot \rho \cdot A \cdot C_p \cdot V^3$$

where :

$$\begin{aligned} \rho &= \text{air density} && \text{kg/m}^3 \\ A &= \text{swept area} && \text{m}^2 \\ C_p &= \text{coefficient of wind turbine} \\ V &= \text{wind velocity} && \text{m/sec} \end{aligned}$$

(6)

$$TSR = \frac{\omega_m R}{V} \quad (7)$$

where :

ω_m - rotor speed - mechanical radian /sec
 R - radius of the blade - meter
 V - linear speed of the wind - meter /sec

From equation 6, it is apparent that the power production from the wind turbine can be maximized if the system is operated at $C_{p-target}$. Thus, it is necessary to keep the rotor speed at constant TSR (i.e., at TSR-Target) shown in equation 7.

As the wind speed changes, the rotor speed should be adjusted to follow the change. This is possible with a variable-speed wind turbine. Unfortunately, it is suggested that the wind speed cannot be reliably measured. To avoid using the wind speed, the equation to compute the target power can be revised. By substituting the wind speed V and the C_p , the target power P_{target} can be written in equation 8 or equation 9. It can be seen that the P_{target} is proportional to the cube of the rotor speed.

$$P_{TARGET} = 0.5 \cdot \rho \cdot A \cdot C_{P_{TARGET}} \left[\frac{RADIUS}{TSR_{TARGET}} \right]^3 \omega_m^3 \quad (8)$$

or

$$P_{TARGET} = K_P (RPM)^3 \quad (9)$$

where :

P_{target} - Target power (max C_p)
 $RADIUS$ - Blade Radius m
 ω_m - rotor speed m/sec
 K_P - computed wind turbine data
 RPM - rotor rpm

The mechanical power generated by the wind turbine as a function of RPM for different wind speeds is shown in Figure 4b. The target power as a function of RPM is shown as a solid line on the same graph. It is clear that for any wind speed, there is always a matching rotor speed which operates the system at maximum power. If the controller can successfully follow the changes in wind speed, the wind turbine will generate maximum power at any speed. The generator is treated as an adjustable load by the wind turbine. It can be controlled to optimize the wind turbine characteristic according to equation 8 (solid line in Figure 4b) by controlling the electrical load. Even if the self-excited induction generator can operate in the dashed line (which is lower than the solid line), the energy captured is better than a constant speed wind turbine by $\Delta P1$ and $\Delta P2$ (shown as the dotted line in Figure 4b).

4. Experiment Result

From section 2 the characteristic of a self-excited induction generator is explored and in section 3 the characteristic of a wind turbine is discussed. Based on this information, the experiment is set up. The concepts explained in section 2 show that an induction generator operates in self excitation if the right size of capacitor is installed. The size of capacitor affects the level of excitation thus the available voltage generated by the induction generator. The size of resistive load affects the power taken from the generator. In this experiment, only one set of capacitor size is used. It is intended to show that a self-excited induction generator can be controlled to generate an adjustable load according to equation 8. Thus, for a given wind turbine

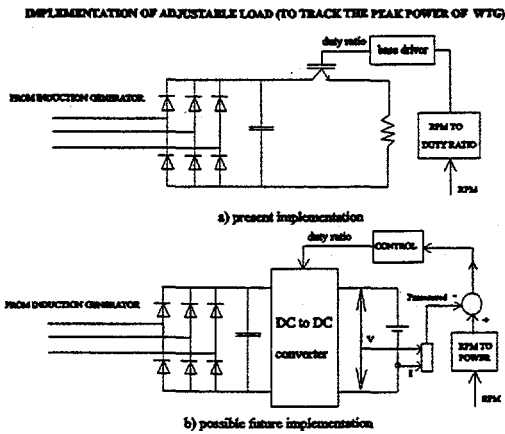


Figure 5. Implementation of adjustable load

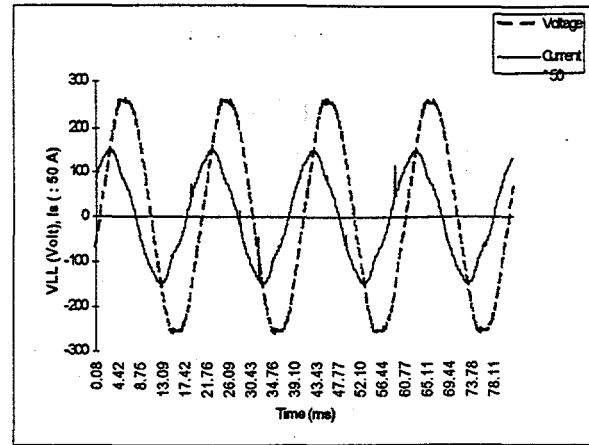


Figure 6. Line voltage and stator current.

characteristic, a self-excited induction generator can be used to operate the wind turbine in variable-speed.

The experiment is set up as shown in Figure 1. An induction machine is connected to a three-phase capacitor and an adjustable resistive load. The resistive load is implemented by a three phase rectifier feeding an adjustable load. In the experiment, the adjustable DC load is implemented as shown in Figure 5a. By controlling the switch at high carrier frequency at different duty ratios, the load reflected to the ac side is an adjustable resistive load. In a battery charging application (as shown in Figure 5b), a DC-DC converter is connected to a DC Battery. The DC-DC converter is controlled to adjust the charging current into the battery. Thus by adjusting the duty ratio of the DC-DC converter, the resulting effect is like adjusting the ac resistive load connected at the terminal of the induction generator.

The wind turbine is assumed to be operated at its maximum C_p all the time. Other operating limits should be handled differently and it is beyond the scope of this paper. It is assumed that we have a wind turbine that will fit the generator under consideration. Using this assumption, the first test conducted in the lab is to determine the K_p factor shown in equation 9 above. The size of capacitor chosen is 60 μF connected in Y or 20 μF connected in Delta. The generator is driven by a dc motor and the maximum power is measured at the rpm limit chosen (which is 1550 rpm). The resistive load is varied until the maximum stator current is reached and at this point the power is recorded as P_{max} . At this limit using the power recorded (P_{max}) and the rotor speed, the K_p factor is determined. Based on the K_p factor determined, a look up table or simple calculation can be performed to compute the power versus RPM for the K_p factor used. The test is then performed by sweeping the RPM and using the look up table provided. In the future, for example in the battery charging application, the system will use RPM feedback as the input to determine the output power required (from look up table or from equation 9). The RPM translates to the required duty ratio of the DC-DC converter. Another way to accomplish the same goal, is to use a close loop feedback and measure the power to be compared to the target power at any rpm, then use the difference between the target power and the measured power to drive the DC-DC converter until the steady state error becomes zero. Using a simple PI controller, this control system can be implemented very easily.

The Table I shown is the data collected in the experiment. From the data collected, the effective ac resistive loads are computed at every step. Using the experimental data (frequency, effective resistive load and ac capacitor value), the steady state solution is computed by using the equivalent circuit approach and the results are compared with the experimental data.

The experiment is based on the power versus rpm requirement (with the assumption that the generator system can be scaled up to an actual wind turbine size). With K_p chosen ($K_p=5.5384E-8$), the generator system is operated to generate the required power. The circuit connection for implementing adjustable load is given in Figure 5. The present implementation (Figure 5a) is a simple adjustable dc load using a single switch operated at three KHz carrier frequency and adjustable duty cycle. The future implementation is shown

in Figure 5b. A sample of voltage and current waveforms are given in Figure 6. The computed airgap voltage is shown in Figure 7, which shows that the airgap voltage increases almost linearly as the frequency increases which means that the flux level is almost the same throughout the experiment. The terminal voltage, as shown in Figure 8, follows the airgap voltage with some reduction due to voltage drop across the stator leakage inductance and stator resistance. The voltage reduction from the airgap voltage becomes more significant as the load increases at higher frequency. The predicted calculation and the experimental data of the terminal voltage is very closely matched. The discrepancy between calculated and experimental data in the higher frequency is caused by the fact that in the real induction generator there are additional core losses and the core loss is a function of the level of the flux and the frequency of operation. In the lower frequency the core loss may be negligible while in the higher frequency it is not.

Table 1. Experimental Data

Rotor Speed (RPM)	Slip (%)	Frequency (Hz)	Line Current (amp)	Line Voltage (volt RMS)	Per phase V (volt RMS)	AC Power (watt)	R_effective (ohm)
1328.12	-4.029	42.556	1.482	129.733	74.901382	129.747	129.7190
1348.30	-4.013	43.209	1.56	137.449	79.356217	134.494	140.4690
1380.71	-3.856	44.315	1.708	148.444	85.704183	146.107	150.8184
1416.88	-3.853	45.477	1.841	158.542	91.534266	157.803	159.2849
1458.49	-3.824	46.826	1.971	167.595	96.761018	167.039	168.1529
1481.62	-3.963	47.505	2.063	172.892	99.819243	176.78	169.0895
1513.01	-4.109	48.443	2.19	180.434	104.17362	190.594	170.8156
1527.72	-4.157	48.892	2.229	181.512	104.796	197.685	166.6622

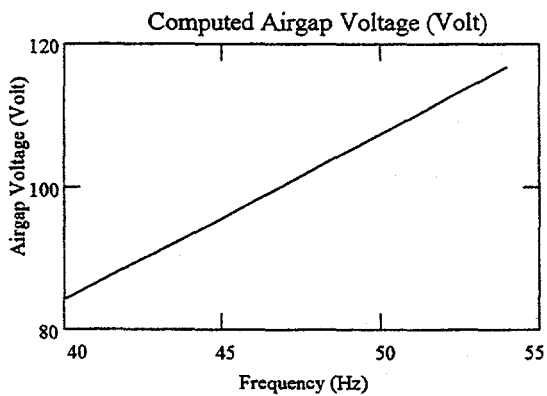


Figure 7. Airgap voltage vs. frequency (Hz)

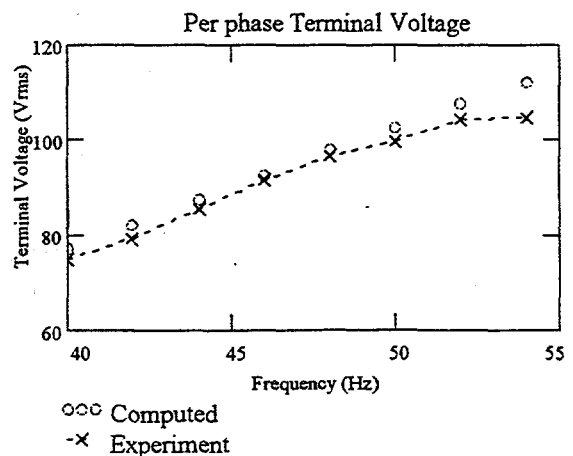


Figure 8. Terminal voltage vs. frequency

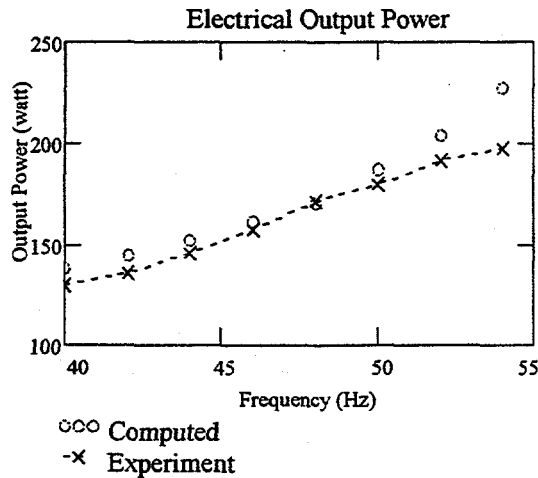


Figure 9. Output power vs. frequency

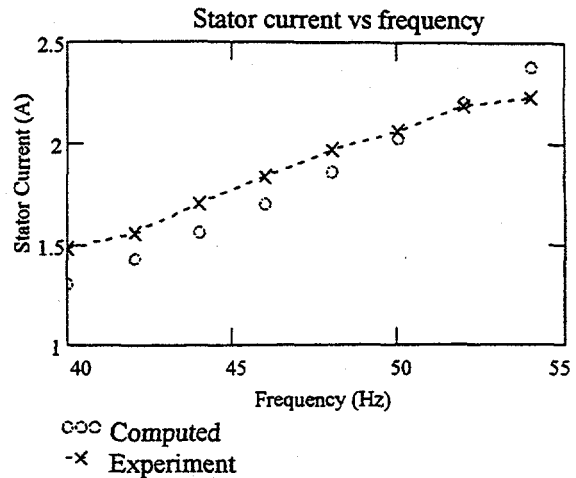


Figure 10. Stator current vs. frequency

In Figure 9, the output power is shown as the frequency varies. This is the output power commanded to achieve maximum C_p operation which is computed based on equation 8 above. The calculated power very closely matches the experiment data. The iron losses which are not modeled in the calculation is shown to be significant in the higher frequency region. The stator current versus frequency as shown in Figure 10. The computed data is very close to the experiment data. At lower frequency the computed data seems to underestimate the experimental data while in the higher frequency, the computed data seems to overestimate the experimental data.

5. Conclusion

Using a self-excited induction generator it is possible to operate the generator across a wider range of rotor speeds. The power can be modulated according to the cube law given in equation 8. Thus with self-excited induction generators, the power can be controlled as such that the maximum C_p operation can be maintained. The core loss (which is omitted in the model) shows a significant effect on the higher frequency. The increase in capacitor size is shown to increase the flux level. Thus it is possible to parallel a second set of capacitors to make the range of operation in the lower frequency wider.

From the discussions presented above, the self-excited induction generator lends itself to operate a variable-speed wind turbine, thus increasing the efficiency of the wind turbine (higher C_p) using a low cost solution. With the correct sizing of capacitors, operation over a wide range of speed can be realized. From the table it is shown that the operation has relatively a constant lower slip, which is related to lower generator loss operation. Although the induction generator used in this experiment is small, the concept can be scaled up to a larger wind turbine size.

ACKNOWLEDGEMENT

The authors wish to thank Diane Broad for assisting in the setting up of the data acquisition systems, collecting data in the lab and preparing the graphs for this paper. They also wish to thank Kristin Tromly from NREL for valuable discussions and for reviewing this manuscript. Thanks to Jerry Bianchi for technical support during the experiment, to Dr. Vahan Gevorgian from National Renewable Energy Lab, Dr. Jan T. Bialasiewicz

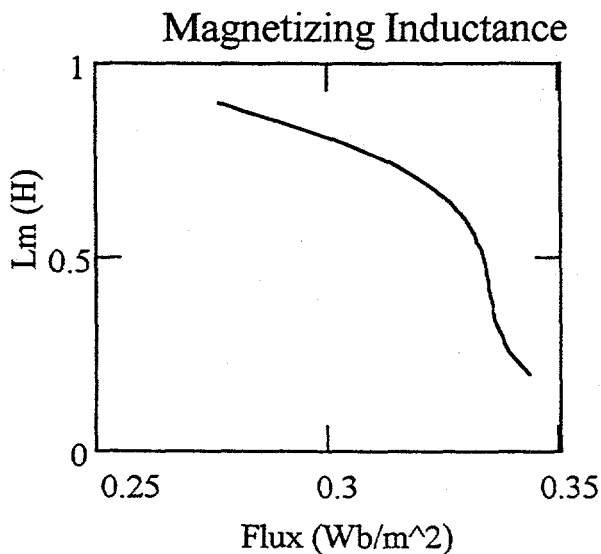
from University of Colorado, Denver, and Dr. Donald Zinger from Northern Illinois University, DeKalb, for valuable technical discussion.

REFERENCES

- [1] C.F. Wagner, "Self Excitation of Induction Motors with Series Capacitors," AIEE Trans., 1941, Vol. 60, pp. 1241-1247.
- [2] L. Quazene and G. McPherson, "Analysis of the Isolated Induction Generator," IEEE Trans. on Power Apparatus and Systems, Vol. PAS 102, No. 8, August 1983, pp. 2793-2798.
- [3] J.A.A. Melkebeek and D.W. Novotny, "Steady State Modelling of Regeneration and Self Excitation in Induction Machines," IEEE Trans. on Power Apparatus and Systems, Vol. PAS-102, No. 8, August. 1983, pp. 2725-2733.
- [4] E. Muljadi, "Series Compensated PWM Inverter with Battery Supply Applied to an Isolated Induction Generator," Ph. D. Thesis, University of Wisconsin, Madison, 1987.
- [5] E. Muljadi, T.A. Lipo and D.W. Novotny, "Power Factor Enhancement of Induction Machine by Means of Solid-State Excitation," IEEE Trans. on Power Electronics, Vol. 4, No. 4, October 1989, pp. 409-418.
- [6] W.J. Hunt, "Steady State Performance of Electronically Self Excited Induction Machine," M.Sc. Thesis, University of Wisconsin, Madison, 1984.
- [7] D.W. Novotny, D.J. Gritter, and G.H. Stuetmann, "Self-excitation in Inverter Driven Induction Machines," IEEE Trans. on Power Apparatus and Systems, No. 4, July/August 1977, pp. 1117-1125.
- [8] E. Muljadi, P.W. Carlin, R.M. Osgood, "Circle Diagram Approach for Self Excited Induction Generators," 1993 North American Power Symposium, Howard University, Oct. 11-Oct.12, 1996.
- [9] E. Muljadi, C.P. Butterfield, "Variable Speed Operation of Generators with Rotor-Speed Feedback in Wind Power Applications," ASME Conference, Houston, Texas, Jan.28-Feb.2, 1996

APPENDIX

Magnetizing Inductance of the Induction Machine



Parameters of induction machine

Squirrel Cage Induction Machine	Parameter Values (at 60 Hz)
1/3 HP, 208 Volts 3 Amps	$R_s = 15.55$ ohms; $R_r' = 17.85$ ohms
1725 rpm (motor)	$X_s = X_r' = 6.3$ ohms